First results from the Nançay timing of the pulsar in the triple system J0337+1715

Guillaume Voisin, LUTh, Observatoire de Paris

6 juillet 2015

With Ismaël Cognard and Lucas Guillemot (LPC2E Orléans)

Introduction

Publication of the discovery of **J0337+1755** by Ransom et al. (2014)

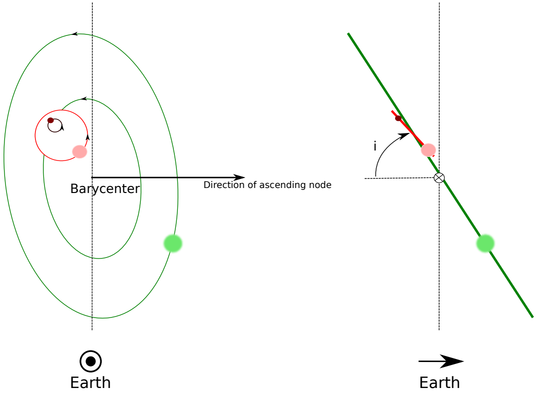

Figure : Sketch of the orbits. The neutron star is the smallest of the bodies but the heaviest so has a smaller amplitude of motion. Together with the closest (red) white dwarf they form the inner system. To a good approximation this one can be considered as a body orbiting the outer (green) white dwarf to form the outer system.

Some characteristics (from Ransom et al. (2014)) :

- Spin period : 2.7 ms; Magnetic field : 10^8Gauss
- Masses : $1.43 M_\odot$ (pulsar), $0.2 M_\odot$ (inner WD), and $0.4 M_\odot$ (outer WD).
- Periods : 1.6 days (inner system), 327 days (outer system)
- Eccentricities : $7 \cdot 10^{-4}$ (inner), $3 \cdot 10^{-2}$ (outer)
- Semi-major axes for the pulsar : 1.9 ls (inner), 118 ls (outer)
- Inclination on the sky : 39°

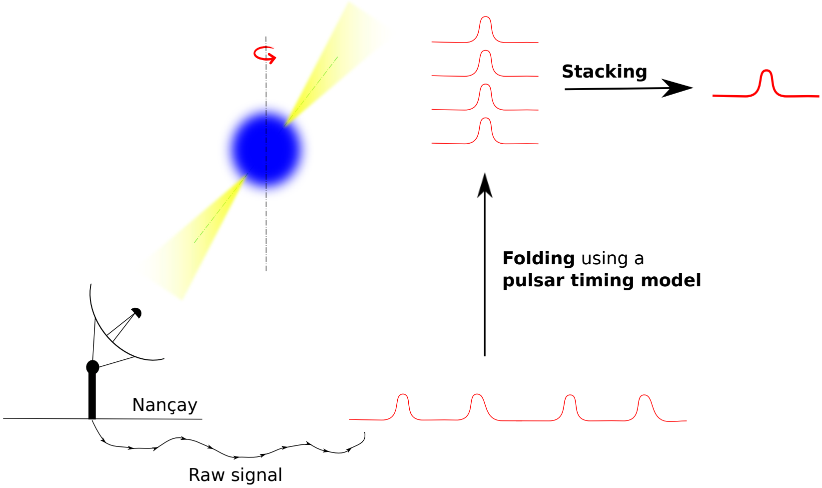

Figure : Principle of pulsar timing

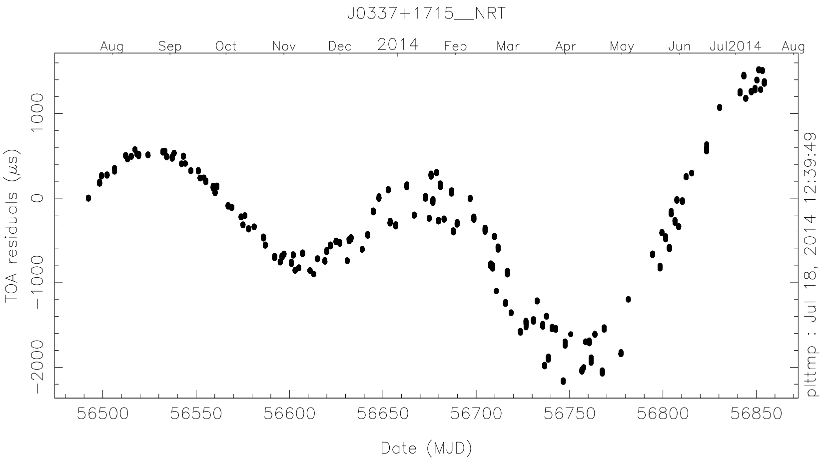

Figure : Residuals of the BTX model applied to the last-to-date Nançay data, that is the difference between the time of arrivals (TOAs) predicted by the model and the measured times.

- In the proper frame of the pulsar, the **timing model** is simple :

$$N(\tau) = N(\tau_0) + f(\tau_0)(\tau - \tau_0) + \frac{1}{2}\frac{\mathrm{d}f}{\mathrm{d}\tau}(\tau_0)(\tau - \tau_0)^2 \qquad (1)$$

τ : proper time.

- But in the Solar-system-barycenter frame, delays come in :

$$N(t_a) = N(t_0) + f(t_0)(\underbrace{t_a - \Delta t}_{\tau} - \tau_0) + \frac{1}{2}\frac{\mathrm{d}f}{\mathrm{d}t}(t_0)(t_a - \Delta t - \tau_0)^2 \qquad (2)$$

t_a : time of arrival in the Solar-system barycenter.

- In the proper frame of the pulsar, the **timing model** is simple :

$$N(\tau) = N(\tau_0) + f(\tau_0)(\tau - \tau_0) + \frac{1}{2}\frac{\mathrm{d}f}{\mathrm{d}\tau}(\tau_0)(\tau - \tau_0)^2 \qquad (1)$$

τ : proper time.

- But in the Solar-system-barycenter frame, delays come in :

$$N(t_a) = N(t_0) + f(t_0)(\underbrace{t_a - \Delta t}_{\tau} - \tau_0) + \frac{1}{2}\frac{\mathrm{d}f}{\mathrm{d}t}(t_0)(t_a - \Delta t - \tau_0)^2 \qquad (2)$$

t_a : time of arrival in the Solar-system barycenter.

Their are numerous delays :

- Rømer delay : geometrical delay due to the propagation of light
- Einstein delay : time dilation due to speed and/or gravitational fields.
- Shapiro delay : light bending and slowing down due to companions.
- Tidal delays : due to tidal interactions
- ...

Their are numerous delays :

- **Rømer delay** : geometrical delay due to the propagation of light
- Einstein delay : time dilation due to speed and/or gravitational fields.
- Shapiro delay : light bending and slowing down due to companions.
- Tidal delays : due to tidal interactions
- ...

Their are numerous delays :

- Rømer delay : geometrical delay due to the propagation of light
- **Einstein delay** : time dilation due to speed and/or gravitational fields.
- **Shapiro delay** : light bending and slowing down due to companions.
- Tidal delays : due to tidal interactions
- ...

Their are numerous delays :

- Rømer delay : geometrical delay due to the propagation of light
- Einstein delay : time dilation due to speed and/or gravitational fields.
- Shapiro delay : light bending and slowing down due to companions.
- **Tidal delays** : due to tidal interactions
- ...

The timing model that was developed

The 3-body Newtonian motion was adressed :

- $$\begin{aligned} k\frac{\mathrm{d}\vec{Q}_I}{\mathrm{d}u} &= \dot{Q}_I && (3)\\ k\frac{\mathrm{d}\dot{\vec{Q}}_I}{\mathrm{d}u} &= -M_J\frac{\vec{Q}_I-\vec{Q}_J}{\|Q_I-Q_J\|^3} - M_K\frac{\vec{Q}_I-\vec{Q}_K}{\|Q_I-Q_K\|^3} && (4)\end{aligned}$$
  and circular permutations of $\{I, J, K\}$.
- Numerical treatment using a Bulirsch-Stoer scheme
- Not periodic as expected from Bertrand's theorem.

The 3-body Newtonian motion was adressed :

- $$k\frac{\mathrm{d}\vec{Q}_I}{\mathrm{d}u} = \dot{Q}_I \qquad (3)$$
  $$k\frac{\mathrm{d}\dot{\vec{Q}}_I}{\mathrm{d}u} = -M_J\frac{\vec{Q}_I-\vec{Q}_J}{\|Q_I-Q_J\|^3} - M_K\frac{\vec{Q}_I-\vec{Q}_K}{\|Q_I-Q_K\|^3} \qquad (4)$$
  and circular permutations of $\{I, J, K\}$.
- Numerical treatment using a Bulirsch-Stoer scheme
- Not periodic as expected from Bertrand's theorem.

The 3-body Newtonian motion was adressed :

- $$\begin{aligned} k\frac{\mathrm{d}\vec{Q}_I}{\mathrm{d}u} &= \dot{Q}_I \qquad (3)\\ k\frac{\mathrm{d}\dot{\vec{Q}}_I}{\mathrm{d}u} &= -M_J\frac{\vec{Q}_I-\vec{Q}_J}{\|Q_I-Q_J\|^3} - M_K\frac{\vec{Q}_I-\vec{Q}_K}{\|Q_I-Q_K\|^3} \qquad (4)\end{aligned}$$
  and circular permutations of $\{I, J, K\}$.
- Numerical treatment using a Bulirsch-Stoer scheme
- Not periodic as expected from Bertrand's theorem.

The Rømer delay is the variation of distance between the observer and the pulsar when it orbits one or several companions

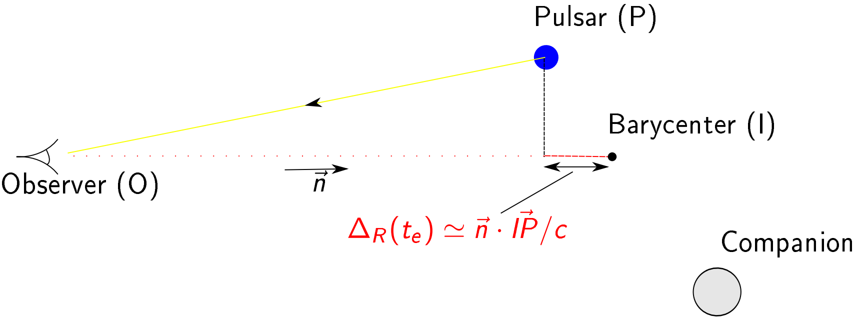

t_e : time of emission in the frame of the observer

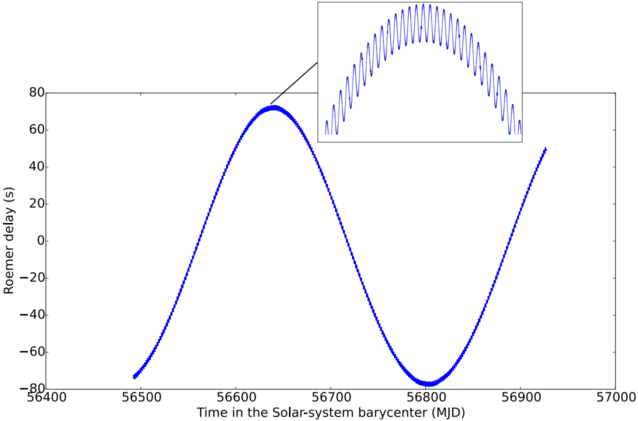

Figure : Rømer delay with second order correction.The large scale curve is mostly due to the presence of the outer companion while the inset shows the modulation due to the inner system.

The Einstein delay is variation of time dilation due to speed and companion gravitational potential variations.

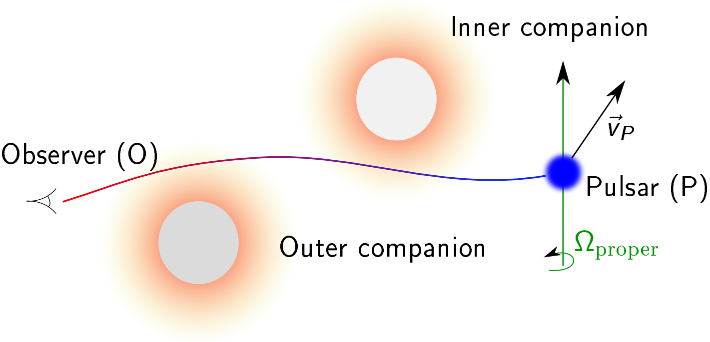

The Shapiro delay is due to the gravitational potential along the light path.

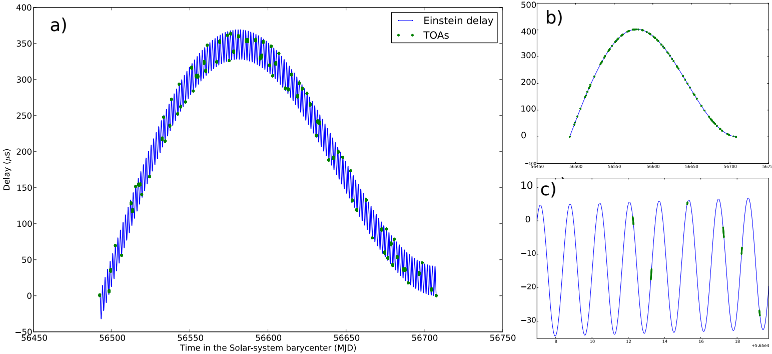

Figure : a) Einstein delay for the parameters drawn from 8-month data (green dots) of J0337 at Nançay, b) Component due to the outer white dwarf during the same time as in a), c) Zoom on the component due to the coupling between the outer and inner speeds. The pseudo-period is that of the inner orbit, about 1.6 days.

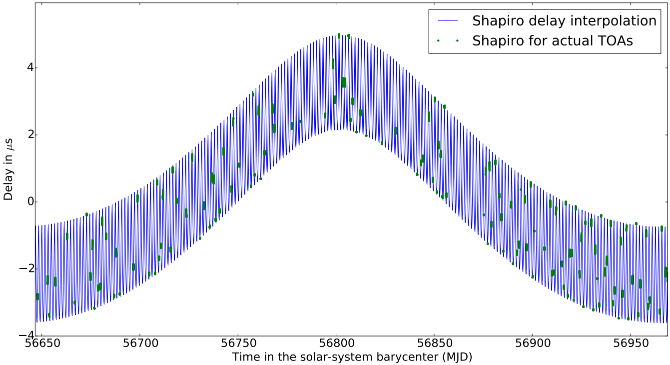

Figure : Shapiro delay for the parameters drawn from 14-month data (green dots) of J0337 at Nançay.

Tidal effects can directly affect the spin frequency of the pulsar.

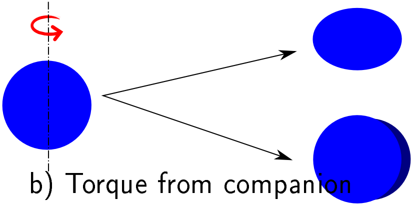

- a) Angular momentum must be conserved.

$$L = I\omega \Rightarrow \delta\omega = -\omega\delta I/I$$

- b) The neutron matter is too stiff (Thorne, 1998).

Tidal effects can directly affect the spin frequency of the pulsar.

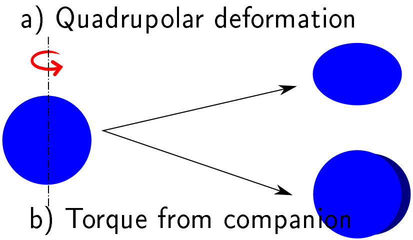

- a) Angular momentum must be conserved.

$$L = I\omega \Rightarrow \delta\omega = -\omega\delta I/I$$

- b) The neutron matter is too stiff (Thorne, 1998).

Let's fit to data !

- **Minuit** is a variable-metric minimizer developed at CERN, suited for many-variable problems.
- We want to find the parameters $\{\theta_k\}$ giving the maximum likelihood for our timing model $N(t_i, \{\theta_k\})$ and turn numbers N_i of uncertainty σ_i :

$$p(D|\{\theta_k\}) = \prod_i \frac{1}{f} \exp \frac{(N(t_i, \{\theta_k\}) - N_i))^2}{2\sigma_i^2} \qquad (5)$$

- Such a fit is not straightforward ! Two tricks were used :
  - Comparison with fake pulsars.
  - Tracking of Minuit steps.

- **Minuit** is a variable-metric minimizer developed at CERN, suited for many-variable problems.
- We want to find the parameters $\{\theta_k\}$ giving the maximum likelihood for our timing model $N(t_i, \{\theta_k\})$ and turn numbers N_i of uncertainty σ_i :

$$p(D|\{\theta_k\}) = \prod_i \frac{1}{f} \exp \frac{(N(t_i, \{\theta_k\}) - N_i))^2}{2\sigma_i^2} \tag{5}$$

- Such a fit is not straightforward ! Two tricks were used :
  - Comparison with fake pulsars.
  - Tracking of Minuit steps.

- **Minuit** is a variable-metric minimizer developed at CERN, suited for many-variable problems.
- We want to find the parameters $\{\theta_k\}$ giving the maximum likelihood for our timing model $N(t_i, \{\theta_k\})$ and turn numbers N_i of uncertainty σ_i :

$$p(D|\{\theta_k\}) = \prod_i \frac{1}{f} \exp \frac{(N(t_i, \{\theta_k\}) - N_i))^2}{2\sigma_i^2} \qquad (5)$$

- Such a fit is not straightforward ! Two tricks were used :
  - Comparison with fake pulsars.
  - Tracking of Minuit steps.

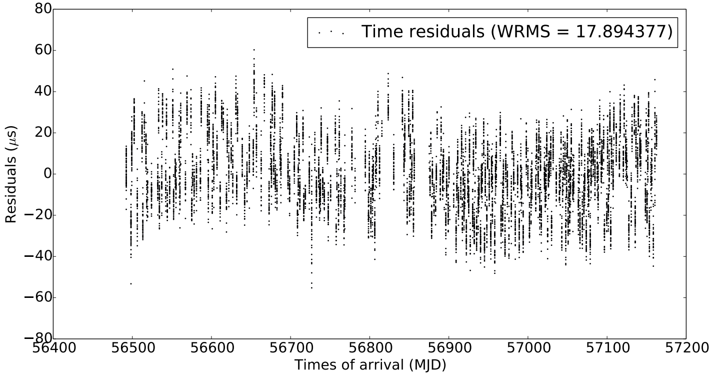

Figure : Best timing residuals obtained so far including Rømer, Einstein and Shapiro delays. It includes 11741 TOAs from Nançay spaning over 670 days.

- We need to **compute the errors** on each parameters. We shall use a Bayesian approach :
- It is generally impossible to compute $p(\{\theta_k\}|D)$. But a Markov-Chain-Monte-Carlo (MCMC) algorithm can draw a sample from this density :
  - Slow but can be parallelized
  - Convergence ensured by the fundamental theorem of Markov chains (Diaconis, 2009).
  - Use of an affine invariant (Goodman and Weare, 2010), more robust, algorithm by Foreman-Mackey et al. (2013).

- We need to **compute the errors** on each parameters. We shall use a Bayesian approach :

$$p(D|\{\theta_k\}) \times p(\{\theta_k\}) = p(\{\theta_k\}|D) \times p(D) \tag{6}$$

- It is generally impossible to compute $p(\{\theta_k\}|D)$. But a Markov-Chain-Monte-Carlo (MCMC) algorithm can draw a sample from this density :
  - Slow but can be parallelized
  - Convergence ensured by the fundamental theorem of Markov chains (Diaconis, 2009).
  - Use of an affine invariant (Goodman and Weare, 2010), more robust, algorithm by Foreman-Mackey et al. (2013).

- We need to **compute the errors** on each parameters. We shall use a Bayesian approach :

$$p(D|\{\theta_k\}) \times p(\{\theta_k\}) = p(\{\theta_k\}|D) \times p(D) \qquad (6)$$

- It is generally impossible to compute $p(\{\theta_k\}|D)$. But a Markov-Chain-Monte-Carlo (MCMC) algorithm can draw a sample from this density :
  - Slow but can be parallelized
  - Convergence ensured by the fundamental theorem of Markov chains (Diaconis, 2009).
  - Use of an affine invariant (Goodman and Weare, 2010), more robust, algorithm by Foreman-Mackey et al. (2013).

- We need to **compute the errors** on each parameters. We shall use a Bayesian approach :

$$p(D|\{\theta_k\}) \times p(\{\theta_k\}) = p(\{\theta_k\}|D) \times p(D) \qquad (6)$$

- It is generally impossible to compute $p(\{\theta_k\}|D)$. But a Markov-Chain-Monte-Carlo (MCMC) algorithm can draw a sample from this density :
  - Slow but can be parallelized
  - Convergence ensured by the fundamental theorem of Markov chains (Diaconis, 2009).
  - Use of an affine invariant (Goodman and Weare, 2010), more robust, algorithm by Foreman-Mackey et al. (2013).

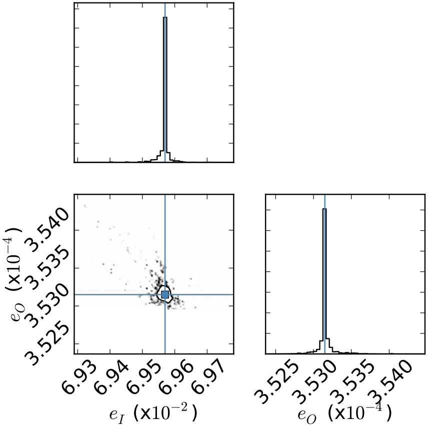

Figure : Statistical distribution of the inner and outer eccentricities as well as their correlation plot. We can see that this last plot is roughly isotropic, and so that the statistical correlation is low, which is the case for all outer parameters with respect to inner parameters, as one might expect. The blue lines show where the fitted value with Minuit is.

Strong equivalence principle test

- Goal : performing a LLR-type experiment on this system ! (Collaboration with P. Freire, N. Wex and M. Kramer (Max-Planck-Institut Für Radioastronomie, Bonn))
- Best tests to date are with pulsar-WD systems :
  - Polarizing field : Sun $6 \cdot 10^{-3} \mathrm{m} \cdot \mathrm{s}^{-2}$ versus Galaxy $2 \cdot 10^{-3} \mathrm{m} \cdot \mathrm{s}^{-2}$
  - Measurement accuracy : 1cm for the Earth-Moon system versus 10m for a pulsar-WD system.
  - $\epsilon_{\mathrm{grav}} = E_{\mathrm{grav}}/M_I c^2$ is $-5 \cdot 10^{-10}$ for Earth versus -0.15 for a neutron star.
- With the triple system : replace the potential of the galaxy by the potential of the outer white dwarf : $0.02 \mathrm{m} \cdot \mathrm{s}^{-2}$! !

- Goal : performing a LLR-type experiment on this system ! (Collaboration with P. Freire, N. Wex and M. Kramer (Max-Planck-Institut Für Radioastronomie, Bonn))
- Best tests to date are with pulsar-WD systems :
  - Polarizing field : Sun $6 \cdot 10^{-3} \mathrm{m} \cdot \mathrm{s}^{-2}$ versus Galaxy $2 \cdot 10^{-3} \mathrm{m} \cdot \mathrm{s}^{-2}$
  - Measurement accuracy : 1cm for the Earth-Moon system versus 10m for a pulsar-WD system.
  - $\epsilon_{\mathrm{grav}} = E_{\mathrm{grav}}/M_I c^2$ is $-5 \cdot 10^{-10}$ for Earth versus -0.15 for a neutron star.
- With the triple system : replace the potential of the galaxy by the potential of the outer white dwarf : $0.02 \mathrm{m} \cdot \mathrm{s}^{-2}$! !

- Goal : performing a LLR-type experiment on this system ! (Collaboration with P. Freire, N. Wex and M. Kramer (Max-Planck-Institut Für Radioastronomie, Bonn))
- Best tests to date are with pulsar-WD systems :
  - Polarizing field : Sun $6 \cdot 10^{-3} \mathrm{m} \cdot \mathrm{s}^{-2}$ versus Galaxy $2 \cdot 10^{-3} \mathrm{m} \cdot \mathrm{s}^{-2}$
  - Measurement accuracy : 1cm for the Earth-Moon system versus 10m for a pulsar-WD system.
  - $\epsilon_{\mathrm{grav}} = E_{\mathrm{grav}}/M_I c^2$ is $-5 \cdot 10^{-10}$ for Earth versus -0.15 for a neutron star.
- With the triple system : replace the potential of the galaxy by the potential of the outer white dwarf : $0.02 \mathrm{m} \cdot \mathrm{s}^{-2}$! !

Conclusion

To conclude :

- A model implementing a full integration of the 3-body Newtonian motion as well as Romer, Einstein and Shapiro delays improves the accuracy by almost two orders of magnitude.
- Tidal effects were investigated and showed no significant contributions.
- The model is not yet complete : Post-Newtonian equations of motion are being implemented.
- Currently starting a collaboration with P. Freire, N. Wex and M. Kramer (Max-Planck-Institut Für Radioastronomie, Bonn) to implement a test of the strong equivalence principle.

To conclude :

- A model implementing a full integration of the 3-body Newtonian motion as well as Romer, Einstein and Shapiro delays improves the accuracy by almost two orders of magnitude.
- Tidal effects were investigated and showed no significant contributions.
- The model is not yet complete : Post-Newtonian equations of motion are being implemented.
- Currently starting a collaboration with P. Freire, N. Wex and M. Kramer (Max-Planck-Institut Für Radioastronomie, Bonn) to implement a test of the strong equivalence principle.

To conclude :

- A model implementing a full integration of the 3-body Newtonian motion as well as Romer, Einstein and Shapiro delays improves the accuracy by almost two orders of magnitude.
- Tidal effects were investigated and showed no significant contributions.
- The model is not yet complete : Post-Newtonian equations of motion are being implemented.
- Currently starting a collaboration with P. Freire, N. Wex and M. Kramer (Max-Planck-Institut Für Radioastronomie, Bonn) to implement a test of the strong equivalence principle.

To conclude :

- A model implementing a full integration of the 3-body Newtonian motion as well as Romer, Einstein and Shapiro delays improves the accuracy by almost two orders of magnitude.
- Tidal effects were investigated and showed no significant contributions.
- The model is not yet complete : Post-Newtonian equations of motion are being implemented.
- Currently starting a collaboration with P. Freire, N. Wex and M. Kramer (Max-Planck-Institut Für Radioastronomie, Bonn) to implement a test of the strong equivalence principle.

To conclude :

- A model implementing a full integration of the 3-body Newtonian motion as well as Romer, Einstein and Shapiro delays improves the accuracy by almost two orders of magnitude.
- Tidal effects were investigated and showed no significant contributions.
- The model is not yet complete : Post-Newtonian equations of motion are being implemented.
- Currently starting a collaboration with P. Freire, N. Wex and M. Kramer (Max-Planck-Institut Für Radioastronomie, Bonn) to implement a test of the strong equivalence principle.

To conclude :

- A model implementing a full integration of the 3-body Newtonian motion as well as Romer, Einstein and Shapiro delays improves the accuracy by almost two orders of magnitude.
- Tidal effects were investigated and showed no significant contributions.
- The model is not yet complete : Post-Newtonian equations of motion are being implemented.
- Currently starting a collaboration with P. Freire, N. Wex and M. Kramer (Max-Planck-Institut Für Radioastronomie, Bonn) to implement a test of the strong equivalence principle.

f (s^{-1})	$365.95332^{+1.4}_{-2.2}$	e_I	$6.9569952^{+2.7}_{-3.2} \cdot 10^{-4}$	e_O	$3.53150^{+1.3}_{-1.2} \cdot 1$
f' (s^{-2})	$-4.443^{+0.73}_{-1.1} \cdot 10^{-14}$	a_p (ls)	$1.2178^{+2.5}_{-3.4}$	a_I (ls)	$74.677^{+5.1}_{-5.0}$
M_p $(M_\odot)$	$1.4325^{+6.1}_{-4.7}$	Ω_p (rad)	$1.6447^{+6.7}_{-8.4}$	Ω_I (rad)	$1.6708^{+4.1}_{-3.5}$
μ_{ip}	$1.0000^{+1.4}_{-1.9}$	T_I(MJD)	$55917.5^{+2.0}_{-7.2}$	T_O (MJD)	$56317.21^{+3.3}_{-2.6}$
μ_{Io}	$1.00000^{+2.6}_{-2.9}$	P_I (days)	$1.6294^{+4.9}_{-5.7}$	P_O (days)	$327.26^{+2.0}_{2.0}$
		i_I (rad)	$1.5483^{+9.6}_{-7.2}$	i_O(rad)	$1.5709^{+5.5}_{-7.9}$

Table : This table shows the best fitted parameters for the 3063 first TOAs from the Nançay decimetric telescope, for the system J0337+1755, with their error bars. The errors are given for the last digit at a 90% confidence level. (ls stands for light-second)

Persi Diaconis. The markov chain monte carlo revolution. *Bulletin of the American Mathematical Society*, 2009.

F. J. Fattoyev, J. Carvajal, W. G. Newton, and Bao-An Li. Constraining the high-density behavior of nuclear symmetry energy with the tidal polarizability of neutron stars. *Physical Review C*, 87(1), January 2013. ISSN 0556-2813, 1089-490X. doi : 10.1103/PhysRevC.87.015806. URL `http://arxiv.org/abs/1210.3402`. arXiv : 1210.3402.

D. Foreman-Mackey, D. W. Hogg, D. Lang, and J. Goodman. emcee : The MCMC Hammer. *Publications of the Astronomical Society of the Pacific*, 125 :306–312, March 2013. doi : 10.1086/670067.

Jonathan M. Goodman and Jonathan Weare. Ensemble samplers with affine invariance. *Communications in Applied Mathematics and Computational Science*, 2010.

Tanja Hinderer. Tidal love numbers of neutron stars. *The Astrophysical Journal*, 677(2) :1216–1220, April 2008. ISSN

Parametrization of the outer orbit :

e_O a_o Ω_O T_O P_O i_O

Intrinsic parameters :

f f' M_p μ_{ip} μ_{Io}

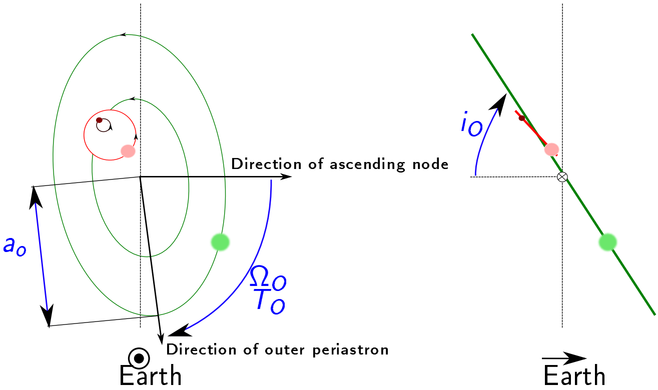

- In the Newtonian limit, the variation of the moment of inertia with respect to the spin axis is related to the **quadrupolar moment** δQ_{xx} of the star along the NS-Companion axis x :

$$\delta I = -\frac{3}{2}\delta Q_{xx} \tag{7}$$

- And δQ_{ij} to the gravitational-field-gradient tensor E_{ij} through the so-called **tidal polarizability** λ (Hinderer (2008) and Fattoyev et al. (2013)) :

$$\delta Q_{ij} = -\lambda E_{ij} \tag{8}$$

- The effect is negligible :

$$\delta\omega \simeq -3.5 \cdot 10^{-15}\mathrm{Hz} \tag{9}$$

- In the Newtonian limit, the variation of the moment of inertia with respect to the spin axis is related to the **quadrupolar moment** δQ_{xx} of the star along the NS-Companion axis x :

$$\delta I = -\frac{3}{2}\delta Q_{xx} \tag{7}$$

- And δQ_{ij} to the gravitational-field-gradient tensor E_{ij} through the so-called **tidal polarizability** λ (Hinderer (2008) and Fattoyev et al. (2013)) :

$$\delta Q_{ij} = -\lambda E_{ij} \tag{8}$$

- The effect is negligible :

$$\delta\omega \simeq -3.5 \cdot 10^{-15}\mathrm{Hz} \tag{9}$$

- In the Newtonian limit, the variation of the moment of inertia with respect to the spin axis is related to the **quadrupolar moment** δQ_{xx} of the star along the NS-Companion axis x :

$$\delta I = -\frac{3}{2}\delta Q_{xx} \tag{7}$$

- And δQ_{ij} to the gravitational-field-gradient tensor E_{ij} through the so-called **tidal polarizability** λ (Hinderer (2008) and Fattoyev et al. (2013)) :

$$\delta Q_{ij} = -\lambda E_{ij} \tag{8}$$

- The effect is negligible :

$$\delta\omega \simeq -3.5 \cdot 10^{-15}\mathrm{Hz} \tag{9}$$

A word about **numerical round-off errors** :

- Data are made of a set of dates, given in Modified Julian Days (MJD).
- Use of 80-bit representation when necessary + systematic check of round-off errors.
- $1\mu\mathrm{s} \sim 300\mathrm{m}$

A word about **numerical round-off errors** :

- Data are made of a set of dates, given in Modified Julian Days (MJD).
- Use of 80-bit representation when necessary + systematic check of round-off errors.
- $1\mu\mathrm{s} \sim 300\mathrm{m}$

A word about **numerical round-off errors** :

- Data are made of a set of dates, given in Modified Julian Days (MJD).
- The first MJD is :

$$56492.29719264059 \tag{10}$$

- Use of 80-bit representation when necessary + systematic check of round-off errors.
- $1\mu\mathrm{s} \sim 300\mathrm{m}$

A word about **numerical round-off errors** :

- Data are made of a set of dates, given in Modified Julian Days (MJD).
- The first MJD is :

$$\underbrace{56492.2971926405\textcolor{red}{9}}_{\text{Maximum length of computer 64-bit representation.}} \tag{10}$$

- Use of 80-bit representation when necessary + systematic check of round-off errors.
- $1\mu\mathrm{s} \sim 300\mathrm{m}$

A word about **numerical round-off errors** :

- Data are made of a set of dates, given in Modified Julian Days (MJD).
- The first MJD is :

$$\underbrace{56492.2971926405\textcolor{red}{9}}_{\text{Maximum length of computer 64-bit representation.}} \tag{10}$$

- Use of 80-bit representation when necessary + systematic check of round-off errors.
- $1\mu\mathrm{s} \sim 300\mathrm{m}$

A word about **numerical round-off errors** :

- Data are made of a set of dates, given in Modified Julian Days (MJD).
- The first MJD is :

$$\underbrace{56492.2971926405\textcolor{red}{9}}_{\text{Maximum length of computer 64-bit representation.}} \tag{10}$$

- Use of 80-bit representation when necessary + systematic check of round-off errors.
- $1\mu\mathrm{s} \sim 300\mathrm{m}$

But only the time of arrival t_a is known :

$$\begin{aligned} \Delta_R(t_e) &= \Delta_R(t_a) \\ &\quad - \Delta_R(t_a)\Delta'_R|_{t_a} \\ &\quad + \left[\Delta_R(t_a)\Delta'_R|^2_{t_a} + \frac{1}{2}\Delta_R(t_a)^2\Delta''_R|_{t_a}\right] \\ &\quad + \circ\left(\frac{\Delta_R}{T}\right)^2 \end{aligned} \tag{11}$$

Where $\Delta_R \lesssim 100$ s and $T \gtrsim 1$ day.

Number of parameters :

The intrinsic parameters μ_{ip} and μ_{Io} :

- $$\mu_{ip} = \frac{m_i^3}{\frac{4\pi^2 a_i^3}{GP_i^2}(m_i + m_p)^2} \tag{12}$$
- With two bodies $\mu_{ip} = 1$: this is Kepler's third law (or mass function).
- With three bodies, μ_{ip} and μ_{Io} are freed because the system is no longer coplanar.

Number of parameters :

$$3 \times 6 \tag{12}$$

The intrinsic parameters μ_{ip} and μ_{lo} :

- $$\mu_{ip} = \frac{m_i^3}{\frac{4\pi^2 a_i^3}{GP_i^2}(m_i + m_p)^2} \tag{13}$$
- With two bodies $\mu_{ip} = 1$: this is Kepler's third law (or mass function).
- With three bodies, μ_{ip} and μ_{lo} are freed because the system is no longer coplanar.

Number of parameters :

$$3 \times 6 + 3 \tag{12}$$

The intrinsic parameters μ_{ip} and μ_{lo} :

- $$\mu_{ip} = \frac{m_i^3}{\frac{4\pi^2 a_i^3}{GP_i^2}(m_i + m_p)^2} \tag{13}$$
- With two bodies $\mu_{ip} = 1$: this is Kepler's third law (or mass function).
- With three bodies, μ_{ip} and μ_{lo} are freed because the system is no longer coplanar.

Number of parameters :

$$3 \times 6 + 3 + 2 \tag{12}$$

The intrinsic parameters μ_{ip} and μ_{lo} :

- $$\mu_{ip} = \frac{m_i^3}{\frac{4\pi^2 a_i^3}{GP_i^2}(m_i + m_p)^2} \tag{13}$$
- With two bodies $\mu_{ip} = 1$: this is Kepler's third law (or mass function).
- With three bodies, μ_{ip} and μ_{lo} are freed because the system is no longer coplanar.

Number of parameters :

$$3 \times 6 + 3 + 2 - 3 \tag{12}$$

The intrinsic parameters μ_{ip} and μ_{Io} :

- $$\mu_{ip} = \frac{m_i^3}{\frac{4\pi^2 a_i^3}{G P_i^2}(m_i + m_p)^2} \tag{13}$$
- With two bodies $\mu_{ip} = 1$: this is Kepler's third law (or mass function).
- With three bodies, μ_{ip} and μ_{Io} are freed because the system is no longer coplanar.

Number of parameters :

$$3 \times 6 + 3 + 2 - 3 - 3 \tag{12}$$

The intrinsic parameters μ_{ip} and μ_{Io} :

- $$\mu_{ip} = \frac{m_i^3}{\frac{4\pi^2 a_i^3}{GP_i^2}(m_i + m_p)^2} \tag{13}$$
- With two bodies $\mu_{ip} = 1$: this is Kepler's third law (or mass function).
- With three bodies, μ_{ip} and μ_{Io} are freed because the system is no longer coplanar.

Number of parameters :

$$3 \times 6 + 3 + 2 - 3 - 3 = 17 \tag{12}$$

The intrinsic parameters μ_{ip} and μ_{Io} :

- $$\mu_{ip} = \frac{m_i^3}{\frac{4\pi^2 a_i^3}{GP_i^2}(m_i + m_p)^2} \tag{13}$$
- With two bodies $\mu_{ip} = 1$: this is Kepler's third law (or mass function).
- With three bodies, μ_{ip} and μ_{Io} are freed because the system is no longer coplanar.

Number of parameters :

$$3 \times 6 + 3 + 2 - 3 - 3 = 17 \qquad (12)$$

The intrinsic parameters μ_{ip} and μ_{lo} :

- $$\mu_{ip} = \frac{m_i^3}{\frac{4\pi^2 a_i^3}{GP_i^2}(m_i + m_p)^2} \qquad (13)$$
- With two bodies $\mu_{ip} = 1$: this is Kepler's third law (or mass function).
- With three bodies, μ_{ip} and μ_{lo} are freed because the system is no longer coplanar.

Number of parameters :

$$3 \times 6 + 3 + 2 - 3 - 3 = 17 \tag{12}$$

The intrinsic parameters μ_{ip} and μ_{Io} :

- $$\mu_{ip} = \frac{m_i^3}{\frac{4\pi^2 a_i^3}{GP_I^2}(m_i + m_p)^2} \tag{13}$$
- With two bodies $\mu_{ip} = 1$: this is Kepler's third law (or mass function).
- With three bodies, μ_{ip} and μ_{Io} are freed because the system is no longer coplanar.

Number of parameters :

$$3 \times 6 + 3 + 2 - 3 - 3 = 17 \tag{12}$$

The intrinsic parameters μ_{ip} and μ_{Io} :

- $$\mu_{ip} = \frac{m_i^3}{\frac{4\pi^2 a_i^3}{GP_I^2}(m_i + m_p)^2} \tag{13}$$
- With two bodies $\mu_{ip} = 1$: this is Kepler's third law (or mass function).
- With three bodies, μ_{ip} and μ_{Io} are freed because the system is no longer coplanar.

Number of parameters :

$$3 \times 6 + 3 + 2 - 3 - 3 = 17 \tag{12}$$

The intrinsic parameters μ_{ip} and μ_{lo} :

- $$\mu_{ip} = \frac{m_i^3}{\frac{4\pi^2 a_i^3}{GP_I^2}(m_i + m_p)^2} \tag{13}$$
- With two bodies $\mu_{ip} = 1$: this is Kepler's third law (or mass function).
- With three bodies, μ_{ip} and μ_{lo} are freed because the system is no longer coplanar.